www.sciencemag.org/cgi/content/full/science.aao3642/DC1

Supplementary Materials for

Arabidopsis pollen tube integrity and sperm release are regulated by RALF-mediated signaling

Zengxiang Ge, Tabata Bergonci, Yuling Zhao, Yanjiao Zou, Shuo Du, Ming-Che Liu, Xingju Luo, Hao Ruan, Liliana E. García-Valencia, Sheng Zhong, Saiying Hou, Qingpei Huang, Luhua Lai, Daniel S. Moura, Hongya Gu, Juan Dong, Hen-Ming Wu, Thomas Dresselhaus, Junyu Xiao, Alice Y. Cheung,* Li-Jia Qu*

*Corresponding author. Email: qulj@pku.edu.cn (L.-J.Q.); acheung@biochem.umass.edu (A.Y.C.)

Published 14 December 2017 on *Science* First Release
DOI: 10.1126/science.aao3642

This PDF file includes:

Other supplementary material for this manuscript includes the following:

Materials and Methods

Plant material and growth conditions

Arabidopsis thaliana (Columbia-0) was used as the wild type (WT). Plants were grown under long-day conditions (16 hr light/ 8 hr dark cycles) at 22±2°C with a light intensity of ～170 μmol/m^2/s using LED bulbs (Philips F17T8/TL841 17 W) (*29*). Arabidopsis were transformed using *Agrobacterium*-mediated floral dip method (*30*).

Phylogenic analysis and transcription assay

The sequences of both CrRLK1L family and RALF family in *Arabidopsis*, can be found in the Arabidopsis Information Resource (http://www.arabidopsis.org/). Accession numbers are as followed:

BUPS1, At4g39110; BUPS2, At2g21480; RALF4, At1g28270; RALF5, At1g35467; RALF14, At2g20660; RALF18, At2g33130; RALF19, At2g33775; RALF24, At3g23805; RALF28, At4g11510; RALF29, At4g11653; RALF31, At4g13950; RALF33, At4g15800; RALF34, At5g67070;

The phylogenetic analysis was performed by using MEGA 5.0 (http://www.megasoftware.net/) and the transcription profile heat-map drawing was based on the RNA-seq data of different tissues. RNA isolation, high-throughput RNA sequencing, bioinformatic and statistical analysis of the RNA-seq data were performed as previously described (*3*, *6*).

Plasmid construction and plant transformation

For GFP reporter assay, genomic sequences of either *BUPS1*, *BUPS2*, *RALF4*, *RALF19* or *RALF34* containing 2 kb promoter sequence and the coding sequence were cloned into a reconstructed vector pK7FWG0, which was developed from pK7FWG2 (Department of Plant Systems Biology, VIB-Ghent University, Ghent, Belgium), by using the pENTR/D-TOPO kit and subsequent LR reaction following the protocol (Invitrogen). For GUS staining assay, 2 kb promoters of *BUPS1*, *BUPS2*, *RALF4*, *RALF19*, *RALF34* were cloned into pB7GUSWG0, in which p35S-RFP-attR1_ccdB_attR2-T35s cassette of pB7WGR2 (Department of Plant Systems Biology,

VIB-Ghent University, Ghent, Belgium) was replaced by attR1_ccdB_attR2-GUS-Tnos from pCB308R cassette (*31*) with caGT FP/RP primers, by using the pENTR/D-TOPO kit and subsequent LR reaction. The constructs were transformed into *Agrobacterium tumefaciens* GV3101 and transformed into wild type (Col-0) and the mutants. Standard PCR-based cloning strategy was used for *BUPS1p::BUPS1-GFP* construction. All the primers for cloning are listed in Table S6.

CRIPSPR/Cas9 and T-DNA induced mutants

In order to obtain the null mutants of *bups1*, *bups2*, *ralf4* and *ralf19*, the egg cell-specific promoter-controlled (EPC) CRISPR/Cas9 system was used as previously reported (*20*, *32*). Briefly, for *bups1* and *bups2*, BUPS_sgRNA1-U6_26t-U6_29p-BUPS_sgRNA2 were amplified from pCBC-DT1T2 by using the primers including the sgRNA sequence and cloned into pHEE401E binary vector, resulting in the production of pHEE401E-BUPS. With aim at knockouting *RALF4* and *RALF19* at the same time, we developed pENTR-MSR vector by cloning the U6_26p-SpR-gRNA_Sc-U6_26t cassette from pHEE401E into pENTR/D-TOPO (Invitrogen) by using primers Topo_KSF and Topo_XHR.

The fragments containing two sgRNAs (*i.e.*, RALF4_sgRNA1-U6_26t-U6_29p-RALF19_sgRNA1 and RALF4_sgRNA2-U6_26t-U6_29p-RALF19_sgRNA2) were subjected for ligation into pENTR-MSR respectively, resulting in the generation of pENTR-R4R19V1 and pENTR-R4R19V2. Next, the pENTR-R4R19V1_V2 was constructed by isocaudamer enzyme-ligation from the two vectors with *Kpn* I/*Spe* I and *Xba* I/*Hin*d III, subsequently amplified with R4-BsF/R19-BsR and cloned into pHEE401E by Golden-Gate Cloning (*33*). The final pHEE401E-R4R19V1_V2 construct was then obtained.

SgRNA sequences mentioned above are as followed:

BUPS_sgRNA1: TAC ACA CAG GAA CAG CTC ANG G

BUPS_sgRNA2: TAT GCT CTT CAG CTT CAA GNG G

RALF4_sgRNA1: AAC GGG CAA GGT TGC ATC GNG G

RALF4_sgRNA2: ACC GTC GTC AAC TCG CAA GNG G

RALF19_sgRNA1: CCG GCG CCA ACT AGC CGC GNG G

RALF19_sgRNA2: TGA CTC GGC GAC TAC AGC CNG G

The two CRISPR constructs were transformed into wild type using *Agrobacterum*-mediated floral dip method respectively (*30*). The mutants were identified by direct sequencing of PCR products of the target in the offspring.

Two T-DNA induced alleles of *bups1*, *bups1-T-1* (SALK_033062) and *bups1-T-2* (FST-430H07) were obtained from Arabidopsis Biological Resource Center (ABRC, Ohio State University, Columbus, OH) and Institut Jean-Pierre Bourgin Resource Center Arabidopsis), respectively. T-DNA insertion and *BUPS1* transcripts was confirmed by genomic PCR and RT-PCR of total flower RNA, respectively, using the primer pairs shown in Table S6.

Pollen assays

For *in vitro* pollen germination assay, pollen grains were dispersed on the PGM (18% sucrose, 0.01% boric acid, 2 mM $CaCl_2$, 1 mM $Ca(NO_3)_2$, 1 mM KCl, 1 mM $MgSO_4$, pH 7.0; 1.5% low-melting point agarose) (*34*, *35*) . Then, the PGM was kept in a humid box for germination at 22°C for 7 hours. Observations were made under a microscope (Olympus BX51, Japan) or a Spinning Disc Confocal Microscopy (Zeiss Cell Observer SD, Zeiss, Germany). The measurement of pollen tube (PT) germination rate, pollen tube length and pollen tube burst percentages were made with Image J software (National Institutes of Health, http://rsbweb.nih.gov/ij/). For Alexander staining (*36*), mature pollen grains were collected from freshly opened flower and treated with Alexander solution directly. For SEM, the pollen shape was observed by a Scanning Electron Microscope (Hitachi S3000N, JOEL JSM-6610).

In vivo pollen tube growth assays

For aniline blue staining, pollen grains were collected from freshly opened flower of wild type or mutant lines, and pollinated to wild-type pistils that had been emasculated 12-24 hours earlier. For limited pollination, countable numbers of pollen grains were deposited. Twenty hours later, siliques were harvested and fixed in acetic acid/ethanol 1:3 for more than two hours. They were washed by 70% ethanol, 50% ethanol, 30%

ethanol and ddH_2O for 10 min each time. After treatment with 8 M NaOH overnight, the pistils with pollen tubes were washed with ddH_2O for three times and stained with aniline blue solution (0.1% aniline blue, 108 mM K_3PO_4) for more than 2 hours (*37*). The stained samples were observed under a fluorescence microscope (Olympus BX51, Japan) equipped with an ultraviolet filter set. Images are representative of more than 20 images captured in each group.

Blue dot assay to assess pollen tube penetration of ovules and rupture to discharge cytoplasm followed described procedure (*38*). Countable numbers of pollen tetrads from *qrt1-2* (a tetrad contains 4 pollen grains and each pollen behaved comparably as WT (*39*)), *bups1-T-1/+ Lat52p::GUS/Lat52p::GUS qrt1-2*, or *bups1-T-2/+ Lat52p::GUS/Lat52p::GUS qrt1-2* was used to pollinate WT pistils. Pistils were processed 24 hours after pollination for GUS histochemical staining.

Flag-tagged ectodomains of BUPS1/BUPS2/ANX1/ANX2 expression and purification in tobacco leaves

In order to obtain the Flag-tagged BUPS1/BUPS2/ANX1/ANX2 ectodomains, the extracellular coding sequences with no stop codon were cloned into pENTR/D-TOPO and introduced into pB7FLAGWG2 (*40*) respectively by LR recombination to generate *p35S::BUPS1-ECD-3×Flag*, *p35S::BUPS2/-ECD-3×Flag*, *p35S::ANX1-ECD-3×Flag* and *p35S::ANX2-ECD-3×Flag* constructs. The expression vectors were transformed into *Agrobacterium tumefaciens* GV3101 and infiltrated into *N. benthamiana* leaves. After incubation in dark for 24 hours and growth under normal condition for 36 hours in a growth chamber, the infiltrated leaves were ground in lysis buffer (50 mM Tris-HCl, pH 8.0, 150 mM NaCl, 10% Glycerol, 5 mM DTT, 1 mM PMSF, 0.5% NP-40, 1xC-complete protease inhibitor (Roche)) on ice. The extracts were centrifuged at top speed (17,000-19,000 g) for 15 min, the supernatant was transferred into a new tube and centrifuged at top speed for another 15 min. The final extracts were incubated with anti-Flag gel (Bimake, B23102) for 4 hours at 4^oC, washed 5 times with the lysis buffer. Then the proteins binding to the gel were eluted with

3xFlag Peptide (Sigma, F4799-4 MG) for 3 times at room temperature and the washes were collected for pull-down assay.

Expression and purification of His-tagged ECDs of BUPS1/2 and ANX1/2

The constructs of BUPS1-ECD, BUPS2-ECD, ANX1-ECD and ANX2-ECD with a C-terminal 6×His tag were generated by standard PCR-based cloning strategy and then were cloned into the pFastBac-Dual vector (Invitrogen) with a modified N-terminal melittin signal peptide. Recombinant baculoviruses were generated and amplified using the Sf21 insect cells maintained in the SIM SF medium. One litre of High Five insect cells (1.5×10^6 cells ml^{-1} cultured in SIM HF medium) was infected with 5 mL recombinant baculovirus. After 48 hours. The medium was harvested and concentrated using a Hydrosart Ultrafilter and exchanged into the binding buffer (25 mM Tris-HCl, pH 8.0, 150 mM NaCl). The proteins were purified with Ni-NTA resin (GE healthcare). Then the bound protein was eluted in buffer containing 25 mM Tris-HCl, pH 8.0, 150 mM NaCl, 500 mM imidazole.

In vitro pull-down assay with biotinylated RALF peptides and ectodomains of BUPS1/BUPS2/ANX1/ANX2

Pull-down assays between RALF peptides and Flag-tagged ectodomains were conducted as described previously (*24*) . In more detail, 10 nM biotin-RALF peptide and 1 ng/μL Flag-tagged proteins were mixed in 500 μL buffer (20 mM Tris-HCl, pH 7.5, 1% IGEPAL) and kept in 4°C for 1 hour. The samples mixed with 50 μL Streptavidin Magnetic Particles (Spherotech, SVMS-30-10) were rotated for 3 hours at 4°C and washed 4-5 times with the buffer. The bound proteins were diluted with SDS-loading buffer and subjected to SDS-PAGE and western blot by using anti-Flag-HRP (Sigma-Aldrich, A8592-2MG).

For the interaction of His-tagged ectodomains with biotinylated RALF peptides, 500 μL of the mixed samples was rotated for 1 hour at 4°C, then incubated with 50 μL Streptavidin Magnetic Particles for another 3 hours at 4°C and washed 4-5 times with the binding buffer. Pull-down was further analyzed with SDS-PAGE and western blot

using α-His antibodies (TransGen Biotech, HT501-02). The competition assay was conducted as described previously (*24*)

MST assay

To test the binding affinity of RALF peptides with the extracellular domains (ECDs), MST assay was conducted by using Monolish NT.115 (NanoTemper Technologies). The His-tagged ectodomains purified from insect cells were labelled according to the manufacturer's procedure. Firstly, the His-tagged proteins were exchanged into a labelling buffer (50 mM NaH_2PO_4/Na_2HPO_4, pH 7.5, 200 mM NaCl, 5% Glycerol, 0.01% Tween 20). The protein concentration was then adjusted to 200 nM with the buffer. Finally, a volume of 90 μL samples was mixed with 90 μL dye solution (100 nM) diluted from the labeling kit (Monolith™ His-Tag Labeling Kit RED-tris-NTA, MO-L008) for 30 min at room temperature. For each assay, the labelled protein mixed with 1 mg/ml BSA was incubated with series of peptide concentration gradients. The samples were loaded into the silica capillaries (Monolith™ NT.115 Standard Treated Capillaries, MO-K002; Monolith™ NT.115 MST Premium Coated Capillaries, MO-K005) and measured by using Monolish NT.115 (NanoTemper Technologies) at medium MST power, 50% or 90% LED power. The data were further analyzed by MO. Affinity Analysis software (V2.2.4).

DUAL membrane yeast two-hybrid

ECDs of BUPS1 and BUPS2 were cloned into GATEWAY-compatible destination vectors pMetycgate-GW bait and the ECDs of ANX1 and ANX2 were cloned into pPR3N-GW prey vector through TOPO and LR reaction (*40*). The bait and prey constructs were co-transformed into yeast strain NMY51 by the lithium acetate transformation method according to the manufacture's procedure (DualmembraneBiotech) for 48 hours. The positive clones were grown on the medium-stringency selective media (-Trp/Leu) and the high-stringency media (-His/Trp/Leu/Ade).

Co-IP experiments

For generation of Co-IP constructs, GATWAY-compatible destination vectors pBA-MYC and pB7FLAGWG2 were used for extracellular domains expression (*40*). The Co-IP experiments were conducted according to a previously reported protocol (*41*). In detail, the ECD coding sequence of ANX1/2 and BUPS1/2 with no stop codon were cloned into pENTR/D-TOPO and introduced into pH7MYCWG2 and pB7FLAGWG2 respectively by LR recombination. The constructs were transformed into *Agrobacterium tumefaciens* GV3101 and co-infiltrated into the leaves of *N. benthamiana* with different combinations. For example *p35S:ANX1-ECD-6×Myc* and *p35S:BUPS1-ECD-3×Flag*, *p35S:ANX2-ECD-6×Myc* and *p35S:BUPS1-ECD-3×Flag*. After incubation for 60 hours, the infiltrated leaves were lysed with the lysis buffer (*see: expression and purification of Flag-tagged ectodomains in tobacco leaves*). The extracts were incubated with anti-c-Myc affinity gel (Sigma, E6654-1 ML) for 3 h at 4°C and washed 5 times with the lysis buffer. The isolated proteins were then separated with SDS-PAGE and analyzed by immunoblot with the corresponding antibodies: anti-Myc (CMCTAG, AT0023) and anti-Flag-HRP (Sigma-Aldrich, A8592-2 MG).

Peptide synthesis and *in vitro* treatment on the pollen tube

All RALF peptides used in this study (Table S5) were synthesized by Scilight Biotechnology LLC (Beijing, China) with a purity higher than 95%. The peptides were diluted into 2 mM with sterile pure water, as reported previously (*26*). For *in vitro* peptide treatment, the dissolved peptide was then diluted with PGM into 2 nM, 20 nM, 200 nM, 2,000 nM and 20,000 nM. Pollen tubes were directly treated with different concentrations of peptides at 7 hours after germination.

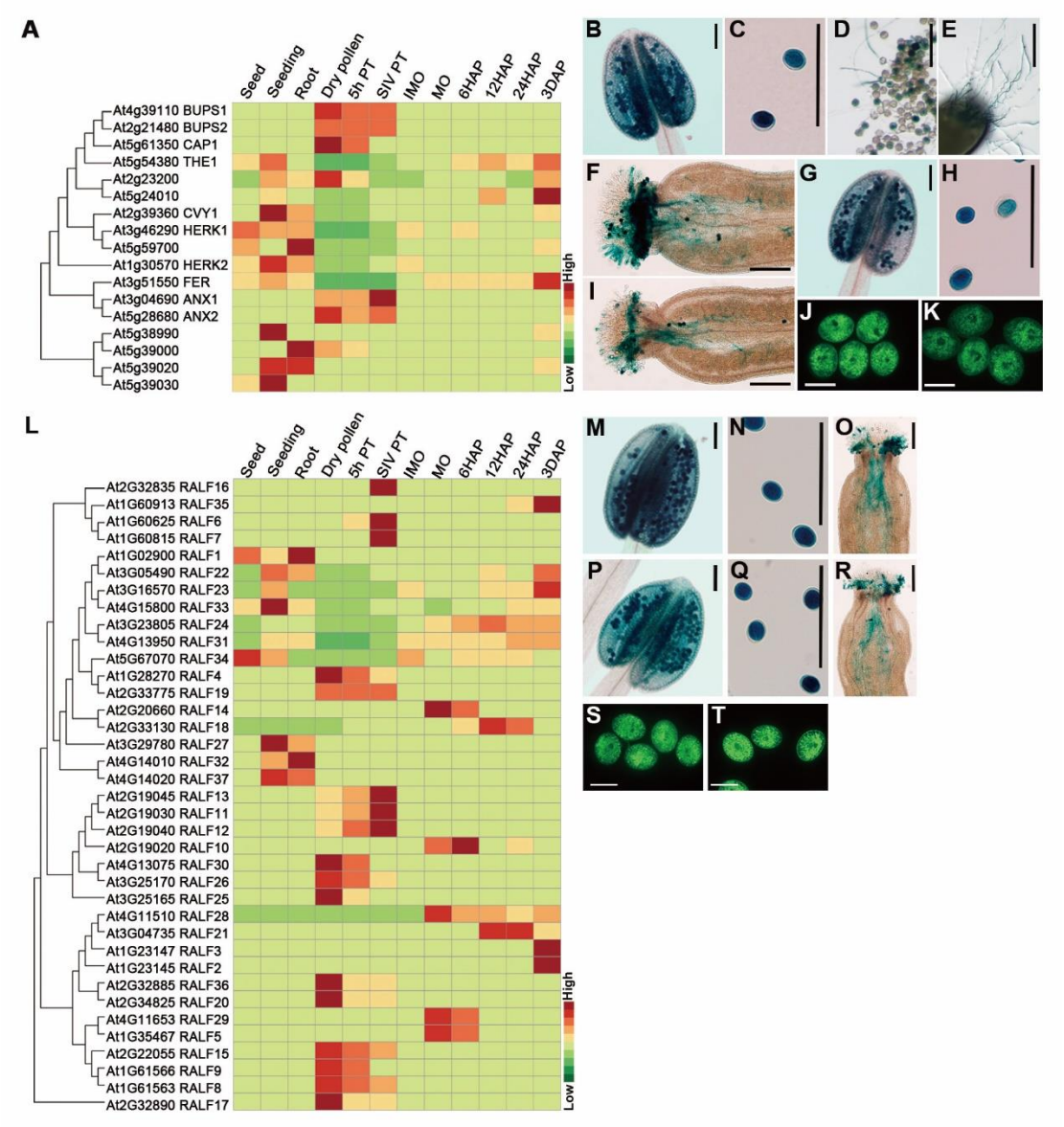

Fig. S1. Expression pattern of CrRLK1L and RALF family members.

(**A)** Heatmap of the CrRLK1L family expression in different tissues. The tree on the left indicates the phylogenetic relations of the 17 members. (**B to I)** Expression pattern of *BUPS1* and *BUPS2*. *BUPS1p::GUS* in anther (**B**), pollen grains (**C**) and pollen tubes (**D to F**, for *in vitro*, semi-*in vivo* and *in vivo* samples), *BUPS2p::GUS* in anther (**G**), pollen grains (**H**) and pollen tube (**I**). Scale bars, 100 μm (**B to E, G and H**) and 200 μm **(F and I)**. Subcellular localization of BUPS1 (**J**) and BUPS2 (**K**) in pollen grains. Scale bars, 20 μm. (**L)** High-throughout RNA-seq analysis of the RALF family in different tissues. The phylogenetic analysis of the 37 members is showed on the left. (**M to R)** Expression pattern of *RALF4* and *RALF19*. *RALF4p::GUS* in anther (**M**),

pollen grains (**N**) and pollen tube (**O**). *RALF19p::GUS* in anther (**P**), pollen grains (**Q**) and pollen tube (**R**). Scale bars, 100 μm (**M, N, P and Q**) and 200 μm (**O and R**). Subcellular localization of RALF4 (**S**) and RALF19 (**T**) in pollen grains. Scale bars, 20 μm.

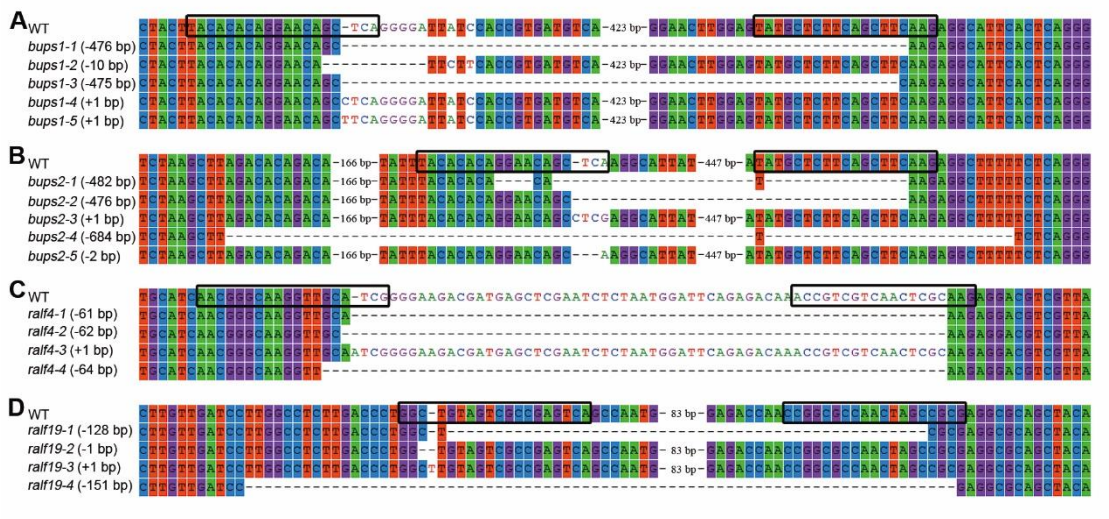

Fig. S2. Mutation analysis of the founders in *BUPS1*, *BUPS2*, *RALF4* and *RALF19*. All the mutations induced by CRISPR/Cas9 were detected by direct sequencing of the PCR products. The inserted (+) or deleted (−) nucleotides are denoted. Sequences framed in black are the sgRNA targets in the gene locus. WT indicates the un-edited sequence of each target gene. The sequence alignment in each group was performed by MEGA5.

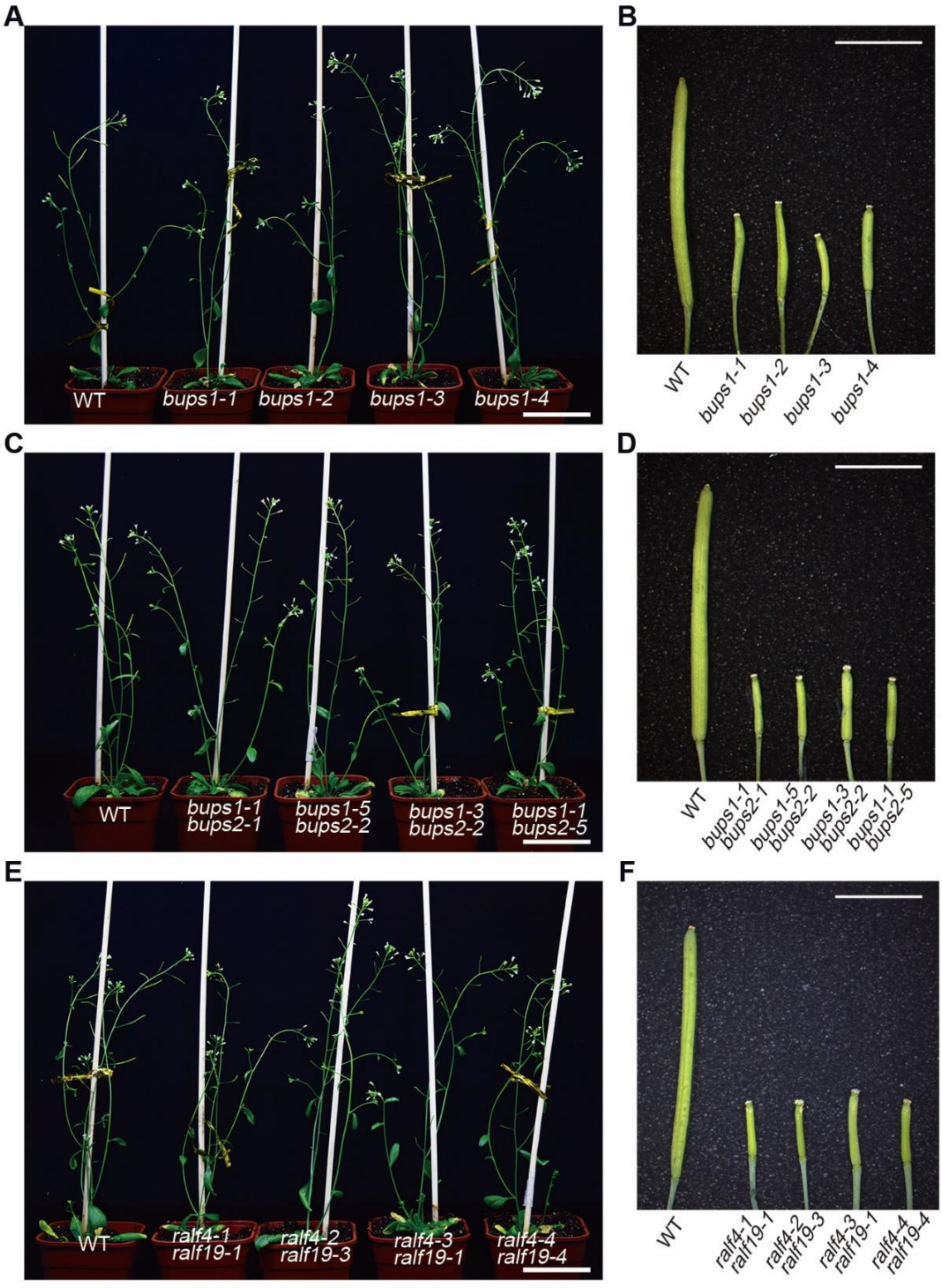

Fig. S3. *bups1, bups1 bups2* and *ralf4 ralf19* exhibit normal vegetative growth but have shorter siliques.

(A, C and E) Vegetative growth of wild-type plant and different *bups1* **(A)**, *bups1 bups*2 **(C)** and *ralf4 ralf19* (**E**) mutant plants. More than 20 plants were observed in each group. Scale bars, 5.00 cm. **(B, D and F)** Comparison of silique length of WT and

mutants of *bups1* **(B)**, *bups1 bups*2 **(D)** and *ralf4 ralf19* **(F)**. The siliques were obtained from self-pollinated plants. Images are representative of about 15 siliques in each group. Scale bars, 5.00 mm.

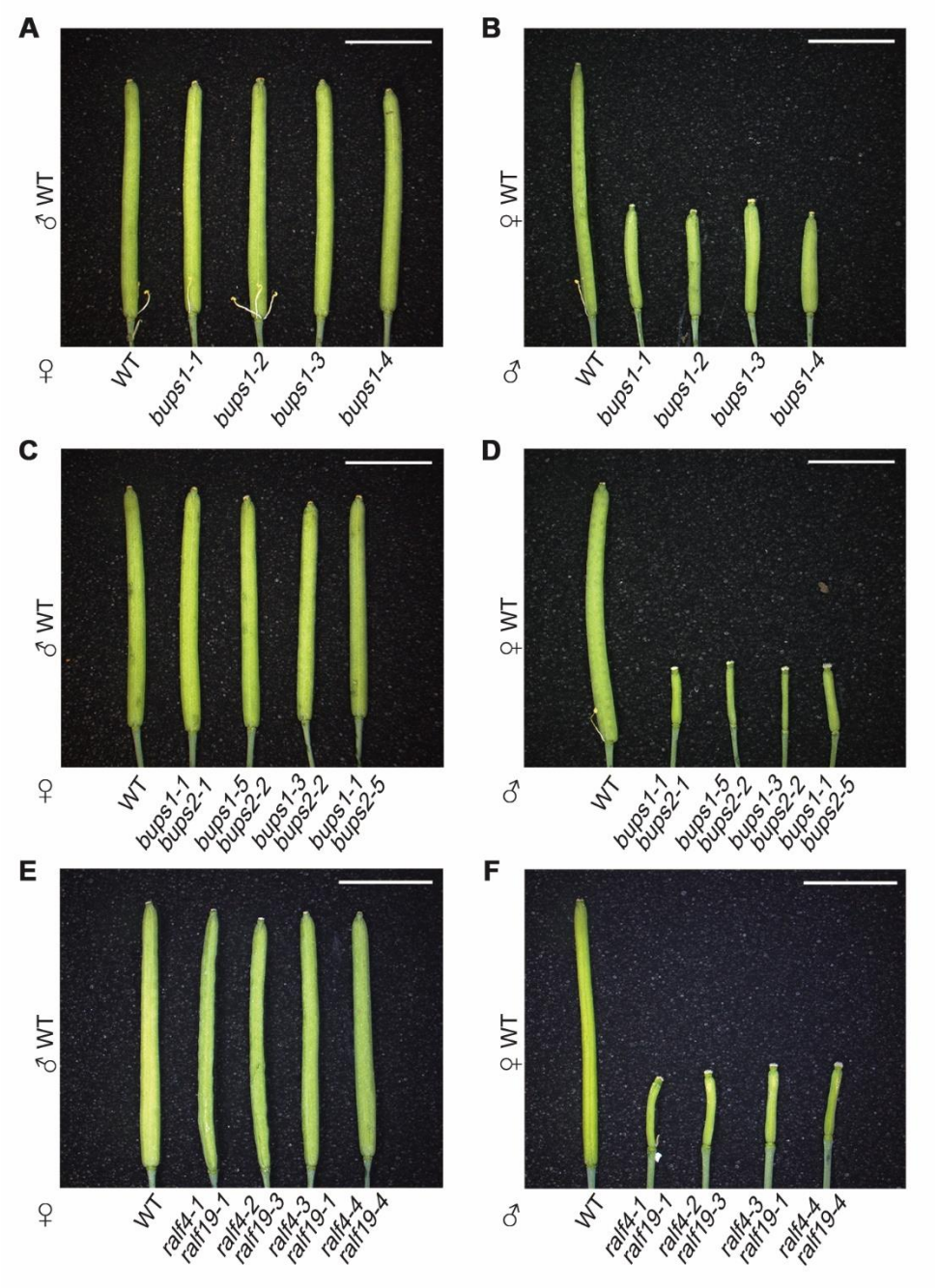

Fig. S4. Fertility defects in *bups1*, *bups1 bups2* and *ralf4 ralf19* are male-specific. **(A, C and E)** Pistils from homozygous *bups1* **(A)**, *bups1 bups2* **(C)** and *ralf4 ralf19* **(E)** were pollinated by WT pollen. (**B, D and F**) WT pistils were pollinated by pollen grains from homozygous *bups1* **(B)**, *bups1 bups*2 **(D)** and *ralf4 ralf19* **(F)**. Siliques were collected after 48 HAP for photography. More than 10 siliques in each group were observed. Scale bars, 5.00 mm.

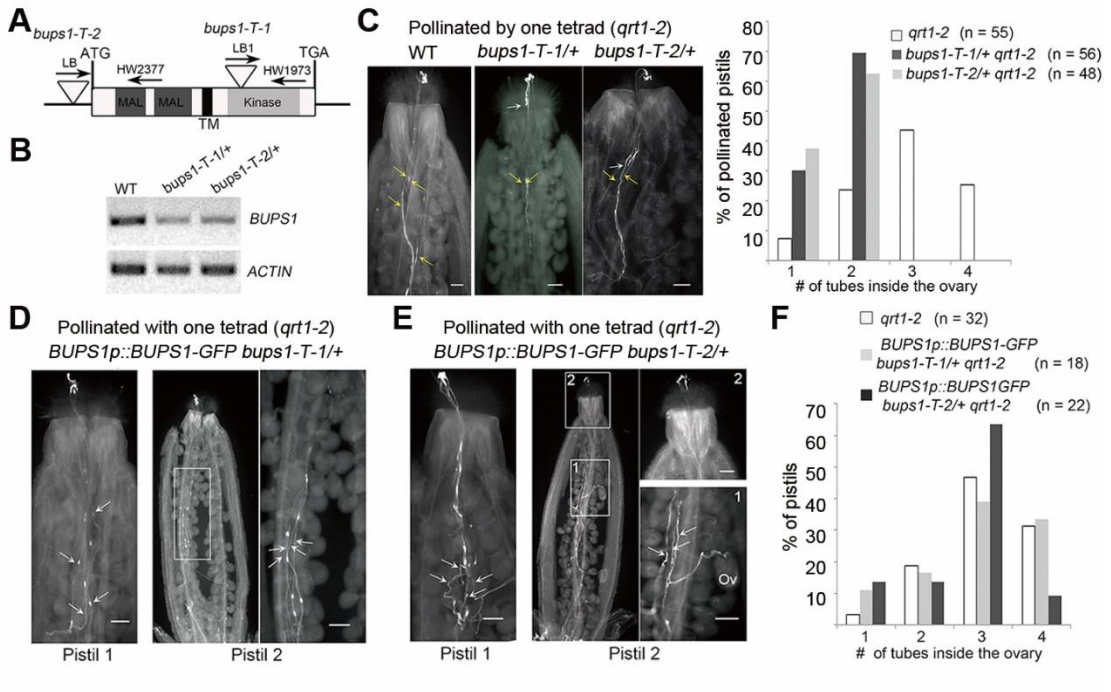

Fig. S5. T-DNA-induced *bups1* alleles result in severe pollen tube growth defects and male deficiency.

(**A**) A schematic representation of T-DNA insertion mutations in *bups1-T-1* and *bups1-T-2*. Triangles, T-DNA insertion sites. Primers (arrows) used for genomic and RT-PCR analysis are shown in Table S6. **(B)** RT-PCR analysis of *BUPS1* transcripts in WT, heterozygous *bups1-T-1* and in *bups1-T-2* flowers. *ACTIN* was used as a reference gene. (**C**) Pollen tubes from heterozygous *bups1-T-1 and bups1-T-2* plants fail to penetrate past the style. Wild type pistils were hand-pollinated by one tetrad from *qrt1-2*, *bups1-T-1*/+ *qrt1-2*, and *bups1-T-2/+ qrt1-2* plants and visualized by aniline blue staining at 20 hours after pollination. Histogram summarizes the distribution of pollen tubes that had grown past the style and entered the ovary chamber. n, number of pollinated pistils. Results demonstrate that no more than two pollen tubes penetrated the ovary cavity when a single heterozygous *bups1* tetrad was used for pollination. Yellow arrows indicate the area that WT pollen tubes arrive and the white indicate that of the mutant pollen tube. (**D and E**) BUPS1-GFP restores *bups1* pollen tube growth to the ovary. Pistils were hand-pollinated by a tetrad of *BUPS1::BUPS1-GFP* transformed *bups1-T-1*/+ *qrt1-2* (**D**) or *BUPS1::BUPS1-GFP* transformed *bups1-T-2*/+

qrt1-2 (**E**). Two representative pistils (1 and 2) are shown for each complemented mutant lines. Boxed area (in **D**) and boxes 1, 2 (in **E**) are shown enlarged on the right to highlight the pollen tubes that had entered the ovary cavity (arrows). Scale bars, 100 μm. (**F**) Distribution of pollen tubes from WT and complemented *bups1* tetrads that had grown past the style and entered the ovary chamber. Results indicate that BUPS1-GFP restores the competence of *bups1* pollen tubes to grow into the ovary, even reaching the ovules (ov).

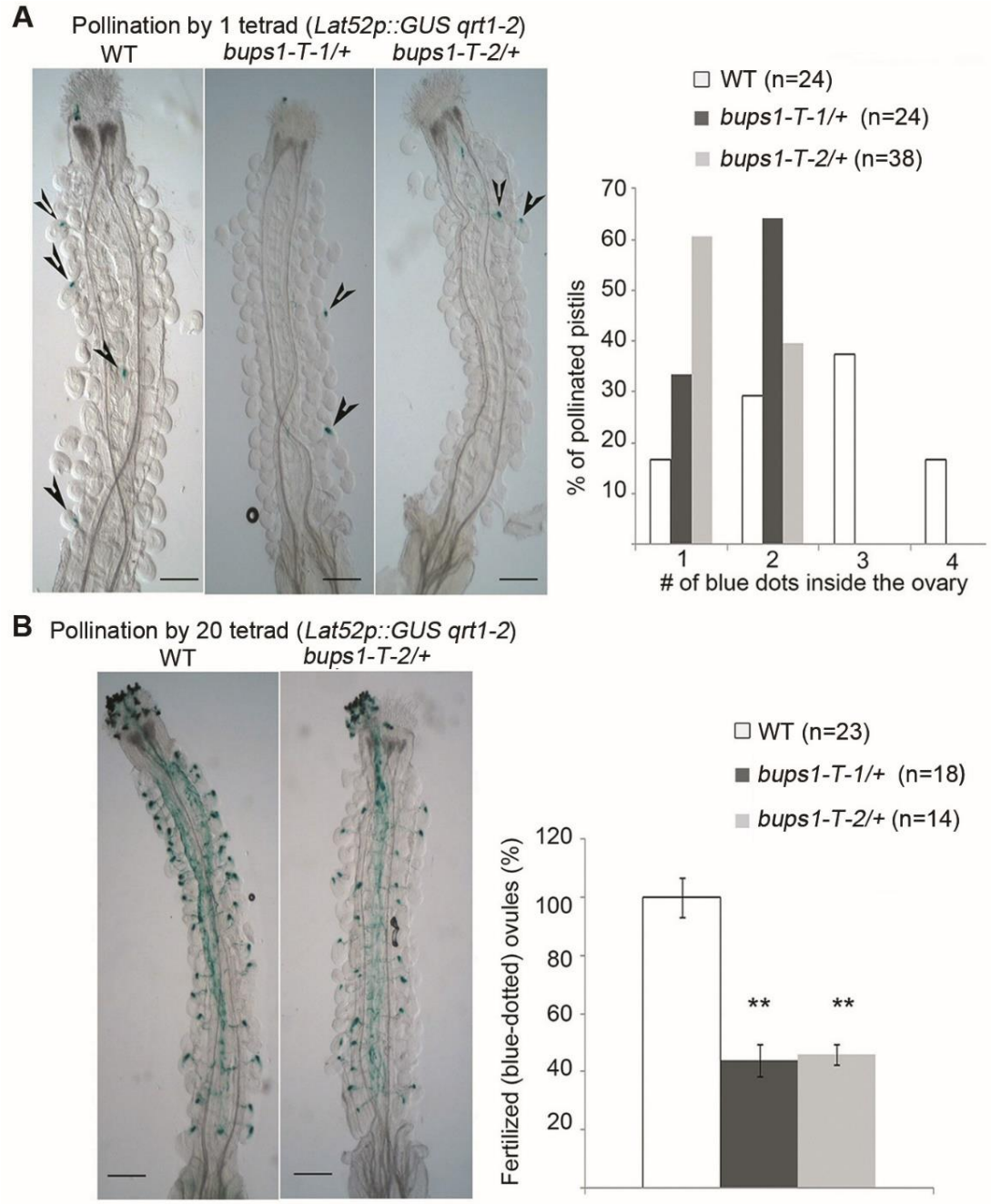

Fig. S6. *bups1* pollen tubes fail to reach the ovules to contribute to fertilization.

(**A and B**) Growth of pollen tubes from WT, *bups1-T-1/+* and *bups1-T-2* (all in *Lat52p::GUS qrt1-2* background) in WT pistils was visualized by "Blue-dot" assays. Each pistil was hand-pollinated by a single tetrad (**A**) or by 20 tetrads (**B**) from WT and *bups1/+* plants as indicated. Arrowheads indicate GUS activity (seen as blue dots) inside ovules reflecting successful arrival of a pollen tube at these ovules and discharge of their cytoplasm inside the female gametophyte. Histograms on right compare the efficiency of pollen tube arrival at the ovules. **, significantly different from WT, $p <$

10^{-15} (*bups1-T-1/+*) and < 10^{-12} (*bups1-T-2/+*) by students' T-test. Scales bars, 250 μm. Results demonstrate that no more than two ovules in pistils pollinated by a single *bups1* tetrad were fertilized (**A**), and when pollinated by 20 tetrads (80 pollen grains), WT pollen cytoplasm occupied close to 100% of the ovules whereas only half the ovules were penetrated by pollen from *bups1/+* tetrads (**B**).

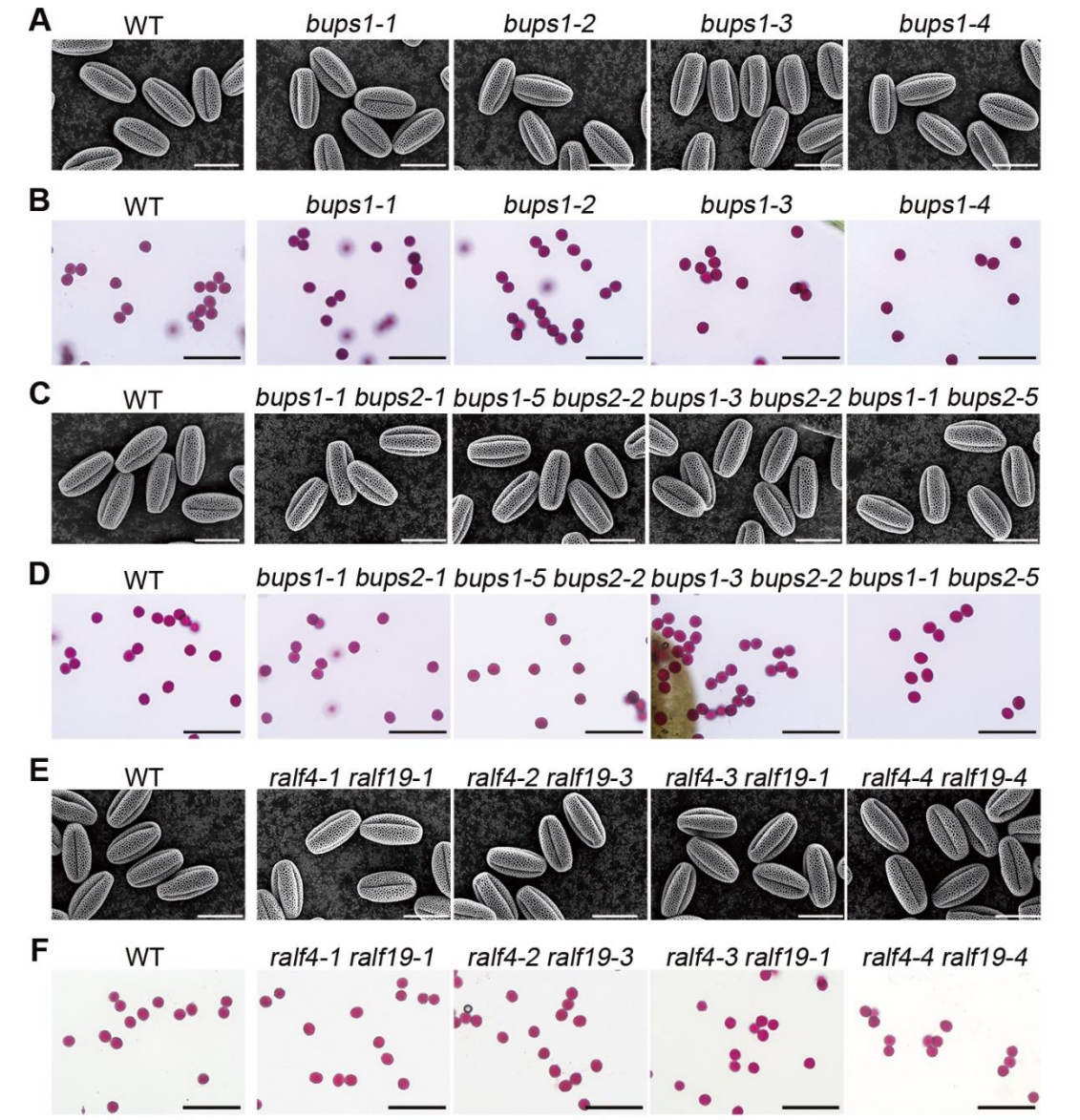

Fig. S7.Morphological analysis of *bups1*, *bups1 bups2* and *ralf4 ralf19* pollen grains.

(A, C and E) Scanning electron microscope (SEM) of pollen grains of *bups1* (**A**), *bups1 bups*2 (**C**) and *ralf4 ralf19* (**E**). Scale bars, 20 μm. **(B, D and F)** Alexander staining of *bups1* (**B**), *bups1 bups*2 (**D**) and *ralf4 ralf19* (**F**) pollen grains. Scale bars, 100 μm. In these assays, mature pollen grains were collected from freshly opened flower to observe the morphology and viability of pollen.

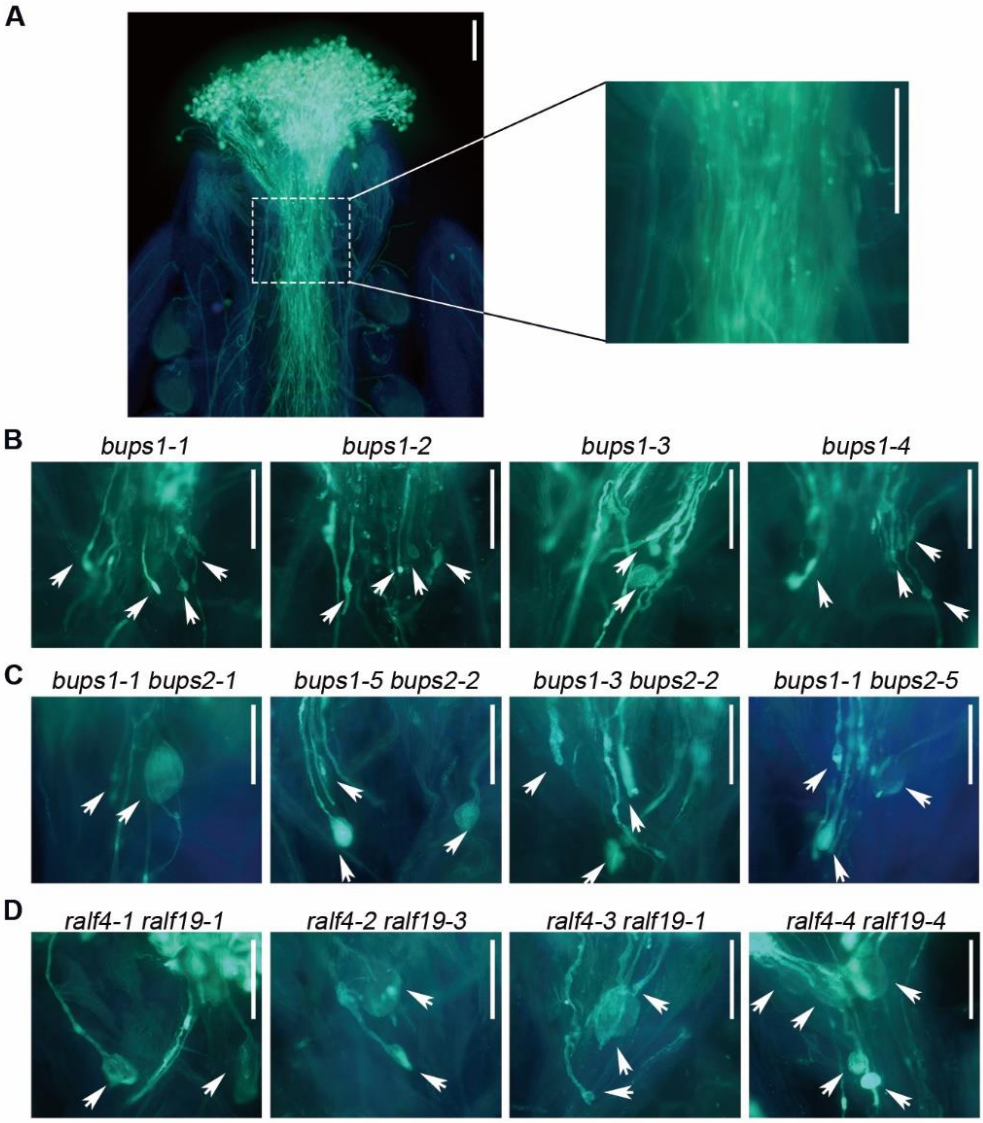

Fig. S8. Aniline blue staining of wild type pistils pollinated with wild type, *bups1*, *bups1 bups2* and *ralf4 ralf19* pollen grains.

(A) Images of WT pollen tube in the WT pistils. High magnification of the boxed area is shown on the right. **(B to D)** High magnification of *bups1* **(B)**, *bups1 bups2* **(C)** and *ralf4 ralf19* (**D**) Pollen tubes in the wild type pistils. Pistils were collected to perform aniline blue staining after twenty hours pollination. Arrows indicate the abnormal tip of pollen tubes. Images were representative of more than 10 samples for each allele. Scale bars, 100 μm.

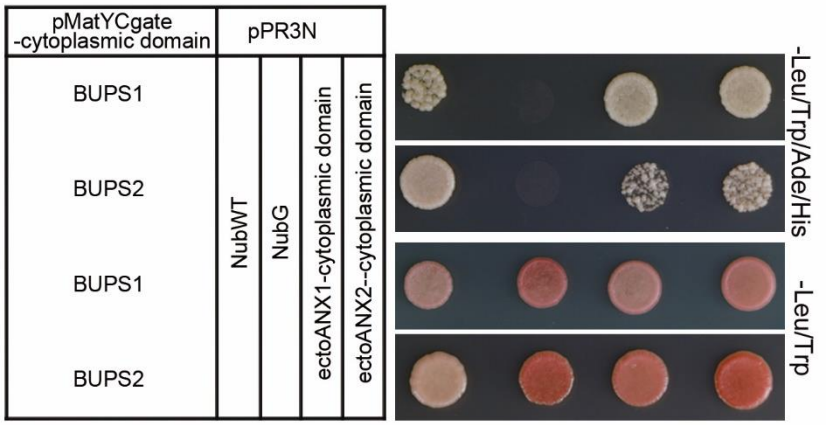

Fig. S9. Interaction analysis between ANX1/2 cytoplasmic domain and BUPS1/2 cytoplasmic domain by Y2H assay.

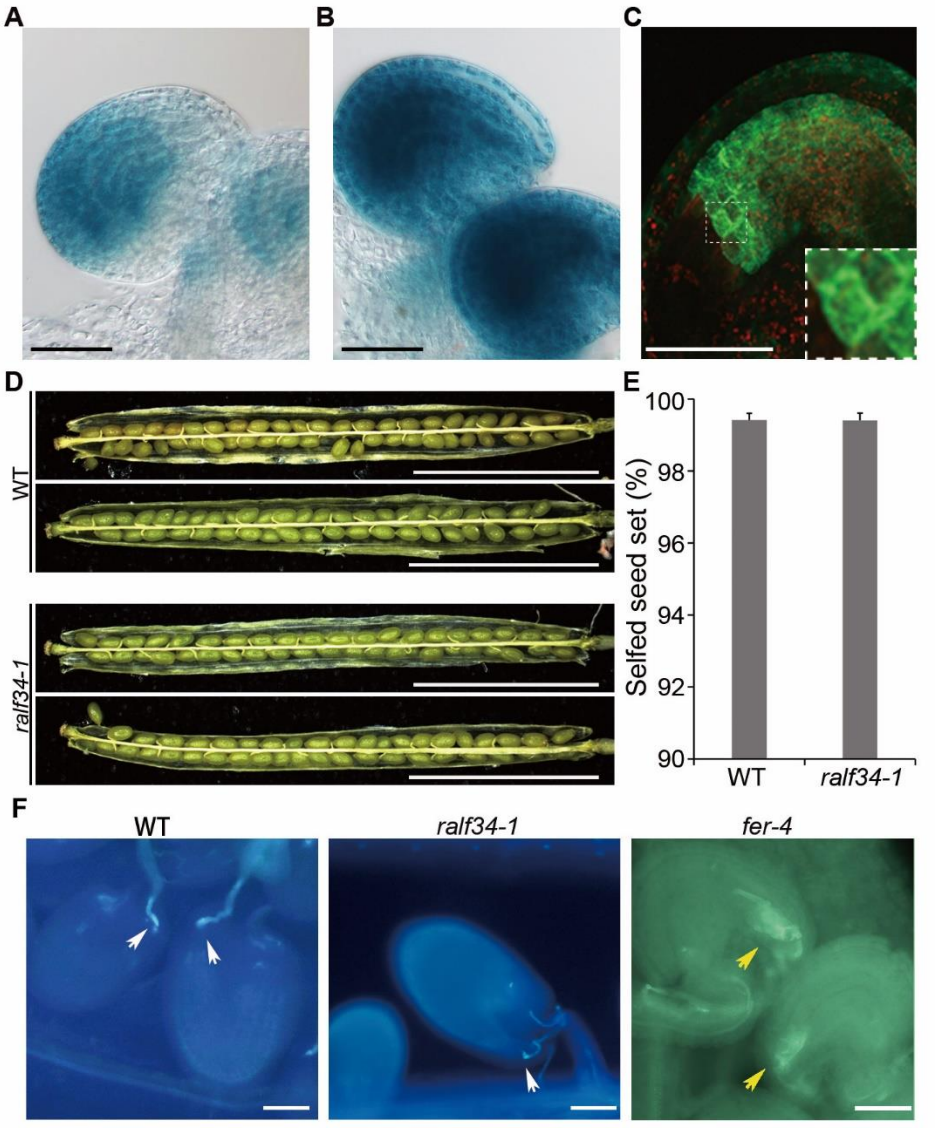

Fig. S10. Ovule expression of *RALF34* and reproductive phenotype of *ralf34-1*.

(A and B) Promoter activity of *RALF34* with GUS staining. Under-stained **(A)** and over-stained ovules **(B)** are shown. Scale bars, 100 μm. **(C)** RALF34-GFP accumulation pattern in the ovules. Dashed box shows a zoom in view of two cells from the ovule to highlight cytoplasmic retention of the fusion protein. Scale bars, 50 μm. **(D to F)** Phenotypic analysis of *ralf34-1* mutant. Overview of developing seeds in a silique **(D)** and statistical analysis of seed set from selfed plants **(E).** Scale bars, 5 mm. n=510 ovules. **(F)** Aniline blue staining of wild type, *ralf34-1* and *fer-4* ovules. White arrows show the normal pollen tube growth; yellow arrows indicate overgrown pollen tubes inside *fer-4* ovules for comparison. Scale bars, 50 μm.

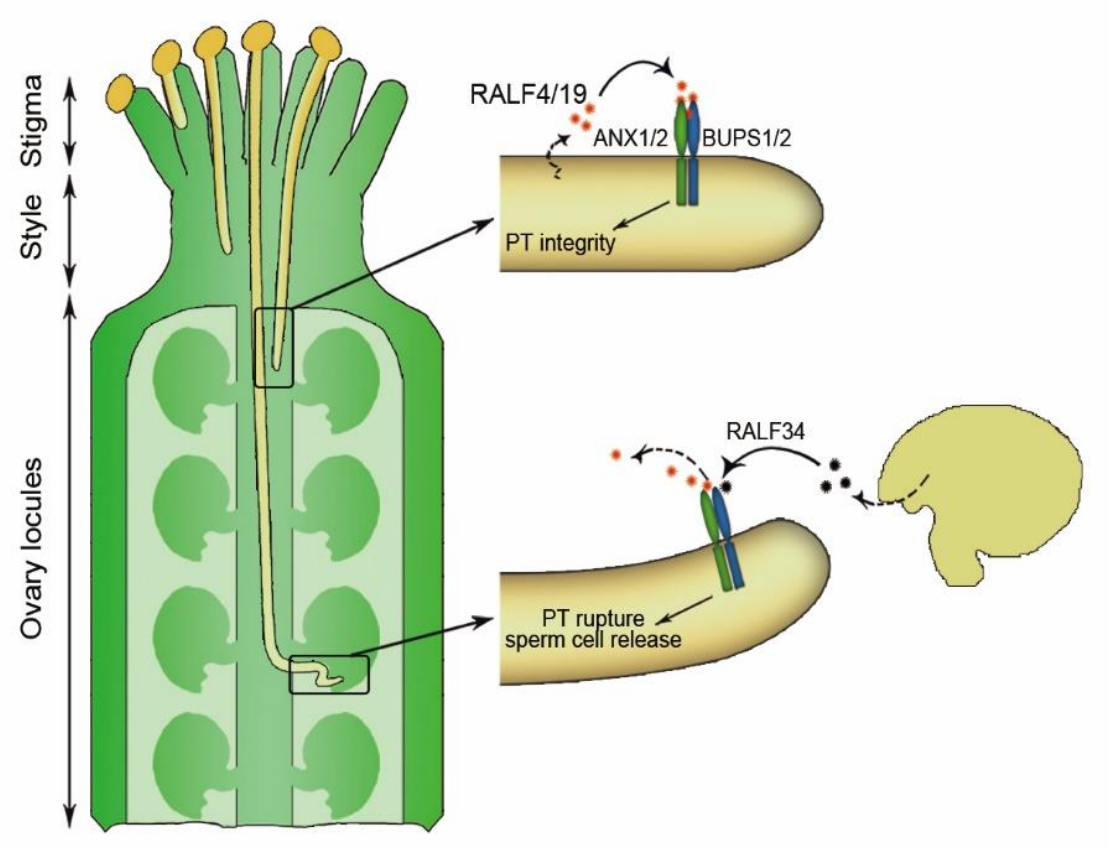

Fig. S11. Model for BUPS1/2-ANX1/2-RALF regulation of pollen tube integrity and sperm cell release.

During the tip growth process in the maternal tissue, pollen-specific BUPS1/2-ANX1/2 receptor heteromer positively regulate pollen tube integrity by perceiving pollen tube-secreted autocrine signal peptides RALF4 and RALF19. Once arriving at the synergid cell surface, female tissue generated peptides, *e.g.*, RALF34, displace the pollen RALFs and bind to the BUPS-ANXUR receptor heteromer in a paracrine fashion leading to pollen tube rupture to release sperm cells for fertilization. PT, pollen tube;

Table S1 Segregation analysis of CRISPR/Cas9-free *bups1*, *bups2*, *bups1 bups2* by PCR-based genotyping in reciprocal crosses.

NA, not applicable; TEf, transmission efficiency of female gametophyte; TEm, transmission efficiency of male gametophyte. X^2 was calculated based on the segregation ratio 1:1 in reciprocal crosses between mutants and wild-type plants.

Female	Male	Number of progeny of each genotype		TEf %	TEm %	p Value
		BUPS1/BUPS1	***bups1/BUPS1***			
bups1-1/BUPS1	**WT**	149	150	99.3	NA	1.00
WT	***bups1-1/BUPS1***	229	3	NA	1.3	2.22E-49
		BUPS2/BUPS2	***bups2/BUPS2***			
bups2-1/BUPS2	**WT**	128	125	102.4	NA	0.90
WT	***bups2-1/BUPS2***	124	102	NA	82.3	0.16
		BUPS1/BUPS1 bups2-1/BUPS2	***bups1/BUPS1 bups2-1/BUPS2***			
bups1-1/BUPS1 bups2-1/bups2-1	**WT**	149	143	104.2	NA	0.77
WT	***bups1-1/BUPS1 bups2-1/bups2-1***	245	0	NA	0.0	8.70E-55

Table S2. **Genetic analyses of T-DNA induced *bups1* mutants**

(A) *bups1-T-1* and *bups1-T-2* are severely male-deficient. Transmission of the *bup1s-T* alleles to progeny was determined by genomic PCR.

Female	Male	WT : *BUPS1/bups1*: *bups1*		Number of progeny analyzed	X^2
		observed	expected		
bups1-T-1/+	***bups1-T-1/+****	1.2:1:0	1:2:1	n = 242	140.4
WT	***bups1-T-1/+***	1:0:0	1:1:0	n = 73	73
bups1-T-1/+	**WT**	1:1.1:0	1:1:0	n = 78	0.21
bups1-T-1/+	***bups1-T-1/+***	1:1.2:0	1:2:1	n = 97	45.2
bups1-T-2/+	***bups1-T-2/+****	1:1.1:0	1:2:1	n = 219	116.8
WT	***bups1-T-2/+***	1:0:0	1:1:0	n = 104	104
bups1-T-2/+	**WT**	1:1:0	1:1:0	n = 198	0.02

X^2 values were tested based on the observed and expected values of segregation among progeny seedlings.
*Natural self-pollination.
**Hand self-pollination, by limited pollen, n = 50-100 grains. Limited pollination minimized the impact from more competitive pollen tubes. Data indicates even when ovules were not occupied by the more competitive wild type pollen tubes, *bups1-T-1* pollen tubes still could not contribute to fertilization.

(B) *BUPS1::BUPS1-GFP* (BUPS1) complements *bups1-T-1* and *bups1-T-2*.

Female	Male	WT[@]	*bups1*[#]	WT : *bups1*		X^2
				(observed)	(expected)	
(BUPS1c) *bups1-T-1/+*	**(BUPS1c) *bups1-T-1/+ ****	8	27	1:3.3	1 : 3**	0.067
WT	**(BUPS1c) *bups1-T-2/+***	7	5	1.4:1	1:1[a]	0
WT	***bups1-T-2/ bups1-T-2***[&]	0	28	0:1	0:1[b]	0

Transmission of the *bups1-T-1* and *bups1-T-2* alleles from BUPS1 transformed (BUPS1c) *bups1-T-1/+* and *bups1-T-2/+* mutants was determined by genomic PCR.

[@]no *bups* T-DNA;

[#]Presence of *bups-1* or *bups-2* T-DNA insert;

*Natural self-pollination;

**If fully complemented, progeny seedlings should segregate 1 WT : 2 *BUPS1/bups1* : 1 *bups1*, so 75% of progeny from self-fertilization should have inherited the *bups1-T-1* T-DNA. Data reflects full complementation.

[&]BUPS1-complemented homozygous *bups1-T-2* mutant

[a]If fully complemented, 50% of progeny should have inherited *bups1-T-2*. Data reflects slight deviation from full complementation, but data set is relatively small.

[b]If fully complemented, 100% of progeny should have inherited *bups1-T-2*. Data indicates 100% of progeny had inherited the T-DNA allele, reflecting full complementation of *bups1-T-2* by BUPS1.

Table S3. Pollen germination and tube growth properties of *bups1, bups2, bups1 bups2* mutant of pollen germination after 7 hours growth *in vitro*.

PT, pollen tube; NA, not applicable.

Genotype	Total pollen germinated	Non-germinated pollen	Intact PTs	PT bursting	PT length(μm)	Pollen germination %	Pollen bursting %
WT	**547**	**195**	**507**	**40**	**268**	**73.7**	**7.3**
bups1-1	**468**	**180**	**24**	**444**	**87**	**72.2**	**94.9**
bups1-2	**468**	**156**	**10**	**458**	**87**	**75.0**	**97.9**
bups1-3	**530**	**202**	**6**	**524**	**93**	**72.4**	**98.9**
bups1-4	**504**	**180**	**4**	**500**	**90**	**73.7**	**99.2**
bups2-1	**450**	**155**	**416**	**34**	**272**	**74.4**	**7.6**
bups2-2	**550**	**210**	**495**	**55**	**253**	**72.4**	**10.0**
bups2-3	**528**	**199**	**497**	**31**	**267**	**72.6**	**5.9**
bups2-4	**546**	**189**	**518**	**28**	**281**	**74.3**	**5.1**
bups1-1 bups2-1	**585**	**168**	**0**	**585**	**NA**	**77.7**	**100.0**
bups1-5 bups2-2	**524**	**122**	**0**	**524**		**81.1**	**100.0**
bups1-3 bups2-2	**517**	**136**	**0**	**517**		**79.2**	**100.0**
bups1-1 bups2-5	**527**	**126**	**0**	**527**		**80.7**	**100.0**

Table S4. Pollen germination and tube growth properties of *ralf4 ralf19* mutant of pollen germination after 7 hours growth *in vitro*.

PT, pollen tube; NA, not applicable.

Genotype	Total pollen germinated	Non-germinated pollen	Intact PTs	PT bursting	PT length (μm)	Pollen germination %	Pollen bursting %
WT	548	185	501	47	261.0	74.8	8.6
ralf4-1 ralf19-1	622	145	0	622	NA	81.1	100.0
ralf4-2 ralf19-3	649	164	0	649		79.8	100.0
ralf4-3 ralf19-1	537	122	0	537		81.5	100.0
ralf4-4 ralf19-4	589	159	0	589		78.7	100.0

Table S5. Peptide sequences used in the study.

Peptide	Sequence
RALF4	ARGRRYIGYDALKKNNVPCSRRGRSYYDCKKRRRNNPYRRGCSAITHCYRYAR
Biotin-RALF4	Biotin-ARGRRYIGYDALKKNNVPCSRRGRSYYDCKKRRRNNPYRRGCSAITHCYRYAR
Biotin-RALF8	Biotin-EASVRYITYPAIDRGDHAVHCDKAHPNTCKKKQANPYRRGCGVLEGCHRETGPKPT
RALF19	AARRSYISYGALRKNNVPCSRRGRSYYDCKKRKRANPYRRGCSVITHCYRQTS
Biotin-RALF19	Biotin-AARRSYISYGALRKNNVPCSRRGRSYYDCKKRKRANPYRRGCSVITHCYRQTS
RALF23	ATRRYISYGALRRNTIPCSRRGASYYNCRRGAQANPYSRGCSAITRCRRS
RALF34	YWRRTKYYISYGALSANRVPCPPRSGRSYYTHNCFRARGPVHPYSRGCSSITRCRR
Biotin-RALF34	Biotin-YWRRTKYYISYGALSANRVPCPPRSGRSYYTHNCFRARGPVHPYSRGCSSITRCRR
Biotin-elf24	Acetyl-SKEKFERTKPHVNVGTIGHVDHGK-biotin

Table S6. Oligo DNA sequence for PCR primers

Purpose	Primer name	Sequence (5'-3')
Subcellular localization observation	BUPS1 full F	CACCATGGAGATAAGAAAGAAACC
	BUPS1 full RNSC	TCTTCCGTTAAGGTTAGCAAAC
	BUPS2 full F	CACCATGGAGATAAGAAAGAAACCAAACATACCC
	BUPS2 full RNSC	TCTTCCGTTAAGGCTAGCAAACTGA
	RALF4 full F	CACCTGCGACGATAAGTACGAGAC
	RALF4 full RNSC	GCGAGCGTACCTATAGCAAT
	RALF19 full F	CACCGTCTTGCACTAGAAACTGGC
	RALF19 full RNSC	AGAAGTTTGCCTGTAGCAATGCG
	RALF34 full F	CACCCATGATGATGCATCAGATGGAGAAGCTT
	RALF34 full RNSC	TCTCCGGCATCGAGTGATCG
Expression pattern analysis	pBUPS1 F	CACCGTCGACATAGAAATTGGTGATTGAAG
	pBUPS1 R	GCGGCCGCCCCTCCTGGGTGGGAAGGAG
	pBUPS2 F	CACCGTCGACGCGACAGGAGTCTCTGCTGGTA
	pBUPS2 R	ACTAGTCCCTCCTTCGTGAAGGGAGA
	pRALF4 F	CACCGGTACCCAGCTGGAAACTGTATTCGCGTTAT
	pRALF4 R	GGATCCTTTGTTTTTTTTTGGTTTTGGTTTTTTAATGAGT
	pRALF19 F	CACCGTCTTGCACTAGAAACTGGC
	pRALF19 R	TTGGTTTTCTTTGTTTTGTTTTGCTGATG
	pRALF34 F	CACCCATGATGATGCATCAGATGGAGAAGCTT
	pRALF34 R	CATGGCGATTGTTGGGGGAA
Ectodomains expression	ANX1 ECD F	CACCATGCAAGATTTAGCTCTGAGCTGC
	ANX1 ECD RSC	TTACTTTTCGTTCTTGAATTCTTTTTTA
	ANX1 ECD RNSC	CTTTTCGTTCTTGAATTCTTTTTTA
	ANX2 ECD F	CACCATGCAAGACATCTCCTTGAGCTGCG
	ANX2 ECD RSC	TTATCTTTTGTCACCTTGAAAGTCCTTTTTAAC
	ANX2 ECD RNSC	TCTTTTGTCACCTTGAAAGTCCTTTTTAAC
	BUPS1 ECD F	CACCATGGGACCTGCTACTGGTTTTAA
	BUPS1 ECD RSC	TTACATACCATGCTTCCCCATGC
	BUPS1 ECD RNSC	CATACCATGCTTCCCCATGC
	BUPS2-ECD F	CACCATGGCCGTCGGTGGTAGCC
	BUPS2 ECD RSC	TTAACCCCTGCTTCCCCATACT
	BUPS2 ECD RNSC	ACCCCTGCTTCCCCATACT
pB7GUSWG0 generation	caGT FP	CCCAAGCTTACAAGTTTGTACAAAAAAGCTGAACGAGA

	caGT RP	CCGGGCCCTTCTCTAGTAACATAGATGACACC
pENTR-MSR construct	Topo KSF	CACCGGTACCACTAGTCGACTTGCCTTCCGCACA ATACATCATTTC
	Topo XHR	GTCGACAAGCTTTCTAGAATAACCATGGTATTGGT TTATCTCATCG
Genotyping for *bups1-T-1*	LB1	GCCTTTTCAGAAATGGATAAATAGCCTTGCTTCC
	HW1973	CGTCGACTTATCTTCCGTTAAGGTTAGC
	HW972	CGTCGACTCTTCCGTTAAGGTTAGCAAACTG
Genotyping for *bups1-T-2*	LB (HW2107)	CGTGTGCCAGGTGCCCACGGAATAGT
	HW2377	CGTCGACATCAGAGATCGGTTCGTCTGG
	HW1677	CGTCGACTACATACCATGCTTCCCCATGCCAG
Genomic analysis for *bups1-T-1*	HW972	CGTCGACTCTTCCGTTAAGGTTAGCAAACTG
	HW973	CGGATCCATGAAGAAGAGGCCACAAGATTGGC
Genomic analysis for *bups1-T-2*	HW1350	GCTGAAACTGTAGATATGGTG
	HW1351	TCCTGGGTGGGAAGGAGAGAG
RT-PCR for BUPS1	HW973	CGGATCCATGAAGAAGAGGCCACAAGATTGGC
	HW1536	TGTCACCACATCAGGCTTAGCGTT
RT-PCR for ACTIN	HW1087	CGTACAACCGGTATTGTGCTGG
	HW1088	GGAGATCCACATCTGCTGGAATG

Movie S1. The movie of *bups1 bups2* pollen tube rupture within 75 min, related to Fig. 1I.

Movie S2. The movie of *ralf4 ralf19* pollen tube rupture within 75 min, related to Fig. 2I.

Movie S3. The movie of pollen tube rupture induced by application of RALF34 (20 μM), related to Fig. 4 (A-F).

References

1. J. Zhang, Q. Huang, S. Zhong, A. Bleckmann, J. Huang, X. Guo, Q. Lin, H. Gu, J. Dong, T. Dresselhaus, L.-J. Qu, Sperm cells are passive cargo of the pollen tube in plant fertilization. *Nat. Plants* **3**, 17079 (2017). doi:10.1038/nplants.2017.79 Medline

2. S. Miyazaki, T. Murata, N. Sakurai-Ozato, M. Kubo, T. Demura, H. Fukuda, M. Hasebe, ANXUR1 and 2, sister genes to FERONIA/SIRENE, are male factors for coordinated fertilization. *Curr. Biol.* **19**, 1327–1331 (2009). doi:10.1016/j.cub.2009.06.064 Medline

3. A. Boisson-Dernier, S. Roy, K. Kritsas, M. A. Grobei, M. Jaciubek, J. I. Schroeder, U. Grossniklaus, Disruption of the pollen-expressed FERONIA homologs ANXUR1 and ANXUR2 triggers pollen tube discharge. *Development* **136**, 3279–3288 (2009). doi:10.1242/dev.040071 Medline

4. T. Wang, L. Liang, Y. Xue, P.-F. Jia, W. Chen, M.-X. Zhang, Y.-C. Wang, H.-J. Li, W.-C. Yang, A receptor heteromer mediates the male perception of female attractants in plants. *Nature* **531**, 241–244 (2016). doi:10.1038/nature16975 Medline

5. H. Takeuchi, T. Higashiyama, Tip-localized receptors control pollen tube growth and LURE sensing in *Arabidopsis*. *Nature* **531**, 245–248 (2016). doi:10.1038/nature17413 Medline

6. J. Liu, S. Zhong, X. Guo, L. Hao, X. Wei, Q. Huang, Y. Hou, J. Shi, C. Wang, H. Gu, L.-J. Qu, Membrane-bound RLCKs LIP1 and LIP2 are essential male factors controlling male-female attraction in *Arabidopsis*. *Curr. Biol.* **23**, 993–998 (2013). doi:10.1016/j.cub.2013.04.043 Medline

7. T. Dresselhaus, S. Sprunck, G. M. Wessel, Fertilization mechanisms in flowering plants. *Curr. Biol.* **26**, R125–R139 (2016). doi:10.1016/j.cub.2015.12.032 Medline

8. L.-J. Qu, L. Li, Z. Lan, T. Dresselhaus, Peptide signalling during the pollen tube journey and double fertilization. *J. Exp. Bot.* **66**, 5139–5150 (2015). doi:10.1093/jxb/erv275 Medline

9. S. Bircheneder, T. Dresselhaus, Why cellular communication during plant reproduction is particularly mediated by CRP signalling. *J. Exp. Bot.* **67**, 4849–4861 (2016). doi:10.1093/jxb/erw271 Medline

10. Q. Huang, T. Dresselhaus, H. Gu, L.-J. Qu, Active role of small peptides in *Arabidopsis* reproduction: Expression evidence. *J. Integr. Plant Biol.* **57**, 518–521 (2015). doi:10.1111/jipb.12356 Medline

11. K. Hématy, P.-E. Sado, A. Van Tuinen, S. Rochange, T. Desnos, S. Balzergue, S. Pelletier, J.-P. Renou, H. Höfte, A receptor-like kinase mediates the response of *Arabidopsis* cells to the inhibition of cellulose synthesis. *Curr. Biol.* **17**, 922–931 (2007). doi:10.1016/j.cub.2007.05.018 Medline

12. H. Guo, L. Li, H. Ye, X. Yu, A. Algreen, Y. Yin, Three related receptor-like kinases are required for optimal cell elongation in *Arabidopsis thaliana*. *Proc. Natl. Acad. Sci. U.S.A.* **106**, 7648–7653 (2009). doi:10.1073/pnas.0812346106 Medline

13. Q. Duan, D. Kita, C. Li, A. Y. Cheung, H.-M. Wu, FERONIA receptor-like kinase regulates RHO GTPase signaling of root hair development. *Proc. Natl. Acad. Sci. U.S.A.* **107**, 17821–17826 (2010). doi:10.1073/pnas.1005366107 Medline

14. L. Bai, X. Ma, G. Zhang, S. Song, Y. Zhou, L. Gao, Y. Miao, C.-P. Song, A Receptor-like kinase mediates ammonium homeostasis and is important for the polar growth of root hairs in *Arabidopsis*. *Plant Cell* **26**, 1497–1511 (2014). doi:10.1105/tpc.114.124586 Medline

15. L. Liu, C. Zheng, B. Kuang, L. Wei, L. Yan, T. Wang, Receptor-like kinase RUPO interacts with potassium transporters to regulate pollen tube growth and integrity in rice. *PLOS Genet.* **12**, e1006085 (2016). doi:10.1371/journal.pgen.1006085 Medline

16. C. Li, H.-M. Wu, A. Y. Cheung, FERONIA and her pals: Functions and mechanisms. *Plant Physiol.* **171**, 2379–2392 (2016). Medline

17. C. X. Pu, Y.-F. Han, S. Zhu, F.-Y. Song, Y. Zhao, C.-Y. Wang, Y.-C. Zhang, Q. Yang, J. Wang, S.-L. Bu, L.-J. Sun, S.-W. Zhang, S.-Q. Zhang, D.-Y. Sun, Y. Sun, The rice receptor-like kinases DWARF AND RUNTISH SPIKELET1 and 2 repress cell death and affect sugar utilization during reproductive development. *Plant Cell* **29**, 70–89 (2017). doi:10.1105/tpc.16.00218 Medline

18. J. M. Escobar-Restrepo, N. Huck, S. Kessler, V. Gagliardini, J. Gheyselinck, W.-C. Yang, U. Grossniklaus, The FERONIA receptor-like kinase mediates male-female interactions during pollen tube reception. *Science* **317**, 656–660 (2007). doi:10.1126/science.1143562 Medline

19. Q. Duan, D. Kita, E. A. Johnson, M. Aggarwal, L. Gates, H. M. Wu, A. Y. Cheung, Reactive oxygen species mediate pollen tube rupture to release sperm for fertilization in *Arabidopsis*. *Nat. Commun.* **5**, 3129 (2014). Medline

20. Z. P. Wang, H.-L. Xing, L. Dong, H.-Y. Zhang, C.-Y. Han, X.-C. Wang, Q.-J. Chen, Egg cell-specific promoter-controlled CRISPR/Cas9 efficiently generates homozygous mutants for multiple target genes in *Arabidopsis* in a single generation. *Genome Biol.* **16**, 144 (2015). doi:10.1186/s13059-015-0715-0 Medline

21. M. Haruta, G. Sabat, K. Stecker, B. B. Minkoff, M. R. Sussman, A peptide hormone and its receptor protein kinase regulate plant cell expansion. *Science* **343**, 408–411 (2014). doi:10.1126/science.1244454 Medline

22. E. Murphy, I. De Smet, Understanding the RALF family: A tale of many species. *Trends Plant Sci.* **19**, 664–671 (2014). doi:10.1016/j.tplants.2014.06.005 Medline

23. K. S. Nissen, W. G. T. Willats, F. G. Malinovsky, Understanding CrRLK1L function: Cell walls and growth control. *Trends Plant Sci.* **21**, 516–527 (2016). doi:10.1016/j.tplants.2015.12.004 Medline

24. M. Stegmann, J. Monaghan, E. Smakowska-Luzan, H. Rovenich, A. Lehner, N. Holton, Y. Belkhadir, C. Zipfel, The receptor kinase FER is a RALF-regulated scaffold controlling plant immune signaling. *Science* **355**, 287–289 (2017). doi:10.1126/science.aal2541 Medline

25. A. Morato do Canto, P. H. O. Ceciliato, B. Ribeiro, F. A. Ortiz Morea, A. A. Franco Garcia, M. C. Silva-Filho, D. S. Moura, Biological activity of nine recombinant AtRALF peptides: Implications for their perception and function in *Arabidopsis*. *Plant Physiol. Biochem.* **75**, 45–54 (2014). doi:10.1016/j.plaphy.2013.12.005 Medline

26. G. Lin, L. Zhang, Z. Han, X. Yang, W. Liu, E. Li, J. Chang, Y. Qi, E. D. Shpak, J. Chai, A receptor-like protein acts as a specificity switch for the regulation of stomatal development. *Genes Dev.* **31**, 927–938 (2017). doi:10.1101/gad.297580.117 Medline

27. W. Tang, D. Kelley, I. Ezcurra, R. Cotter, S. McCormick, LeSTIG1, an extracellular binding partner for the pollen receptor kinases LePRK1 and LePRK2, promotes pollen tube growth *in vitro*. *Plant J.* **39**, 343–353 (2004). doi:10.1111/j.1365-313X.2004.02139.x Medline

28. W. Tang, I. Ezcurra, J. Muschietti, S. McCormick, A cysteine-rich extracellular protein, LAT52, interacts with the extracellular domain of the pollen receptor kinase LePRK2. *Plant Cell* **14**, 2277–2287 (2002). doi:10.1105/tpc.003103 Medline

29. J. Zhang, B. Wei, R. Yuan, J. Wang, M. Ding, Z. Chen, H. Yu, G. Qin, The *Arabidopsis* RING-type E3 ligase TEAR1 controls leaf development by targeting the TIE1 transcriptional repressor for degradation. *Plant Cell* **29**, 243–259 (2017). doi:10.1105/tpc.16.00771 Medline

30. S. J. Clough, A. F. Bent, Floral dip: A simplified method for *Agrobacterium*-mediated transformation of *Arabidopsis thaliana*. *Plant J.* **16**, 735–743 (1998). doi:10.1046/j.1365-313x.1998.00343.x Medline

31. Z. Y. Lei, P. Zhao, M.-J. Cao, R. Cui, X. Chen, L.-Z. Xiong, Q.-F. Zhang, D. J. Oliver, C.-B. Xiang, High-throughput binary vectors for plant gene function analysis. *J. Integr. Plant Biol.* **49**, 556–567 (2007). doi:10.1111/j.1744-7909.2007.00442.x

32. H. L. Xing, L. Dong, Z.-P. Wang, H.-Y. Zhang, C.-Y. Han, B. Liu, X.-C. Wang, Q.-J. Chen, A CRISPR/Cas9 toolkit for multiplex genome editing in plants. *BMC Plant Biol.* **14**, 327 (2014). doi:10.1186/s12870-014-0327-y Medline

33. C. Engler, R. Kandzia, S. Marillonnet, A one pot, one step, precision cloning method with high throughput capability. *PLOS ONE* **3**, e3647 (2008). doi:10.1371/journal.pone.0003647 Medline

34. Y. Hou, X. Guo, P. Cyprys, Y. Zhang, A. Bleckmann, L. Cai, Q. Huang, Y. Luo, H. Gu, T. Dresselhaus, J. Dong, L.-J. Qu, Maternal ENODLs are required for pollen tube reception in *Arabidopsis*. *Curr. Biol.* **26**, 2343–2350 (2016). doi:10.1016/j.cub.2016.06.053 Medline

35. L. C. Boavida, S. McCormick, Temperature as a determinant factor for increased and reproducible in vitro pollen germination in *Arabidopsis thaliana*. *Plant J.* **52**, 570–582 (2007). doi:10.1111/j.1365-313X.2007.03248.x Medline

36. M. P. Alexander, Differential staining of aborted and nonaborted pollen. *Stain Technol.* **44**, 117–122 (1969). doi:10.3109/10520296909063335 Medline

37. T. Mori, H. Kuroiwa, T. Higashiyama, T. Kuroiwa, GENERATIVE CELL SPECIFIC 1 is essential for angiosperm fertilization. *Nat. Cell Biol.* **8**, 64–71 (2006). doi:10.1038/ncb1345 Medline

38. M. A. Johnson, B. Kost, Pollen tube development. *Methods Mol. Biol.* **655**, 155–176 (2010). doi:10.1007/978-1-60761-765-5_11 Medline

39. K. E. Francis, S. Y. Lam, G. P. Copenhaver, Separation of *Arabidopsis* pollen tetrads is regulated by QUARTET1, a pectin methylesterase gene. *Plant Physiol.* **142**, 1004–1013 (2006). doi:10.1104/pp.106.085274 Medline

40. L. Hao, J. Liu, S. Zhong, H. Gu, L.-J. Qu, AtVPS41-mediated endocytic pathway is essential for pollen tube-stigma interaction in *Arabidopsis*. *Proc. Natl. Acad. Sci. U.S.A.* **113**, 6307–6312 (2016). doi:10.1073/pnas.1602757113 Medline

41. J. J. English, G. Davenport, T. Elmayan, H. Vaucheret, D. Baulcombe, Requirement of sense transcription for homology-dependent virus resistance and trans-inactivation. *Plant J.* **12**, 597–603 (1997). doi:10.1046/j.1365-313X.1997.d01-13.x